Machine-learned force fields

18-04-24. 27th Wien2k Workshop. Trieste.

Georg Madsen

Institute of Materials Chemistry, TU Wien, Austria

TECHNISCHE
UNIVERSITÄT
WIEN

Outline

- Neural-network force fields
- Effective harmonic potentials
  - Phase stability in HfO_2
- The $SrTiO_3$ surface phase diagram
- Nested sampling
  - The phase diagram of Si

Machine-learned force fields

Use regression model to bypass explicit calculation of E_{pot}

Descriptor based MLFF:

- Behler-Parinello (2007) and Bartók-Csányi (2010)
- Preprocess structure into symmetry compliant fingerprints
- Map onto energies and forces through ML model

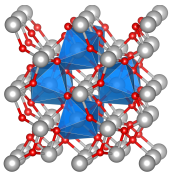

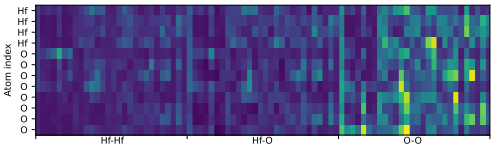

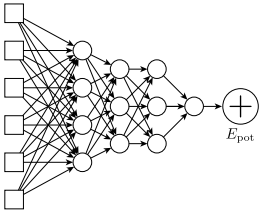

Perceptron

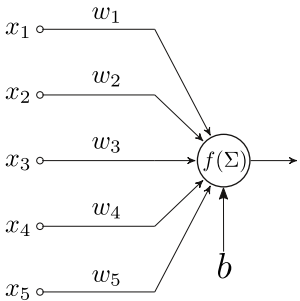

Multi-layer perceptron (Neural network)

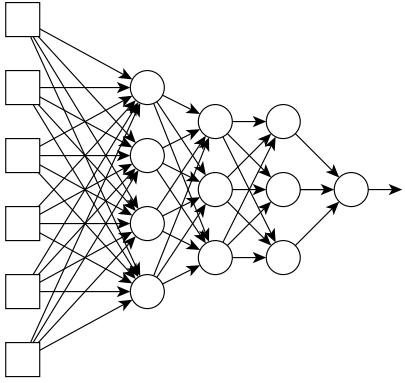

Activation function

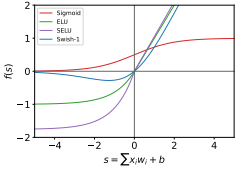

Perceptron

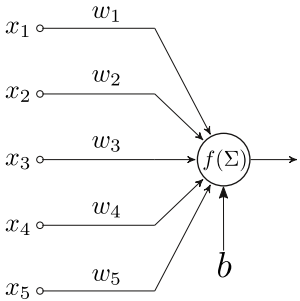

Multi-layer perceptron (Neural network)

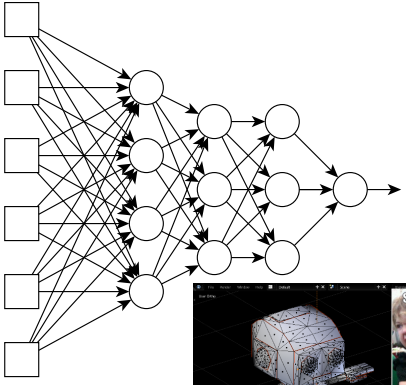

Activation function

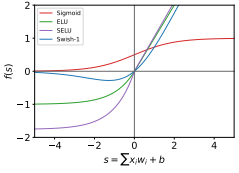

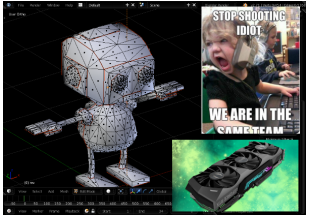

Algorithmically differentiable JAX-based neural-network force field

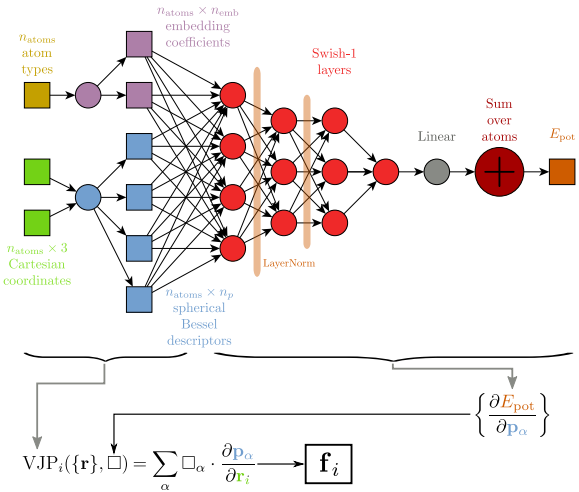

- Just-in-time compilation of Python functions
- Automatic differentiation
-Multiple CPU/GPU/TPU cores

- Swish activation function
- Element-specific-spherical-Bessel fingerprints

Montes-Campos, Carrete, Bichelmaier, Varela, Madsen, *J. Chem. Inf. Model* 62 (2022) p88

Spherical Bessel descriptors

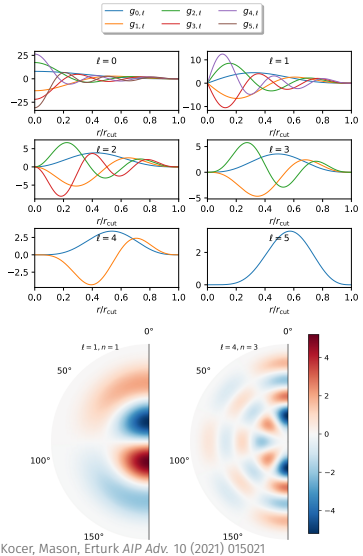

Kocer, Mason, Erturk *AIP Adv.* 10 (2021) 015021

Project weighted local density

$$\rho_i(\boldsymbol{r}) = \sum w_{ij}\delta(\boldsymbol{r} - \boldsymbol{R}_{ij})$$

onto orthonormal basis functions

$$B_{nlm} = g_{n-l,l}(r)Y_l^m(\theta, \varphi)$$

and calculate the power spectrum.

Optimize Completeness

Training. 15 ionic pairs of ethylammonium nitrate

Project local density *of each chemical species*

$$\rho_{ij}(\boldsymbol{r}) = \sum \delta(\boldsymbol{r} - \boldsymbol{R}_{ij})$$

onto orthonormal basis functions

$$B_{nlm} = g_{n-l,l}(r) Y_l^m(\theta, \varphi)$$

Model	MAE E_{pot} (meV/atom)	MAE f meV/Å
ZWEIGHTS	16.9	171
NEURALIL	1.9	65
NEURALIL+CENT	1.9	61

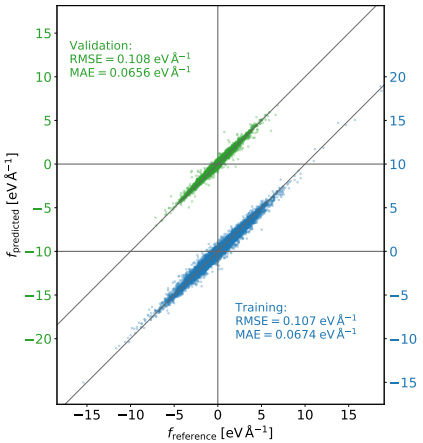

Montes-Campos, Carrete, Bichelmaier, Varela, Madsen, *J. Chem. Inf. Model* 62 (2022) p88

Transferability

Swish activation function

$$s_\beta(x) = \frac{x}{1 + \exp(-\beta x)}$$

Ramachandran, Zoph, Le *arXiv 1710.05941*

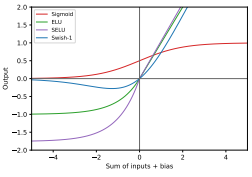

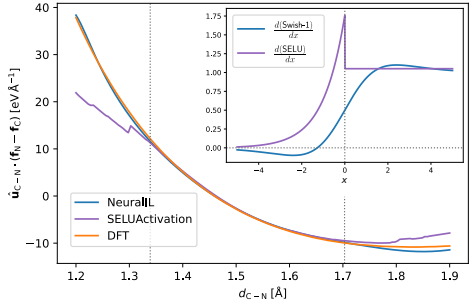

Diffusion coefficients

10^{-11} m^2/s	Exp	OPLS	NeuralIL
D_{anion}	6.9	0.13	8.7
D_{cation}	4.6	0.07	8.2

Montes-Campos, Carrete, Bichelmaier, Varela, Madsen, *J. Chem. Inf. Model* 62 (2022) p88

Outline

- Neural-network force fields
- Effective harmonic potentials
  - Phase stability in HfO_2
- The $SrTiO_3$ surface phase diagram
- Nested sampling
  - The phase diagram of Si

Canonical ensemble

Partition function

$$Z(N,V,T) \propto \sum \exp\left(\frac{-E_{pot}}{k_B T}\right)$$

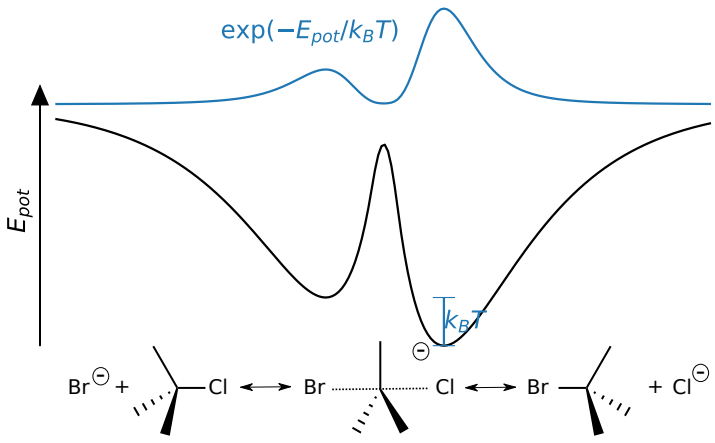

$20^{3.6} = 2.6 \cdot 10^{23}$

Hafnia

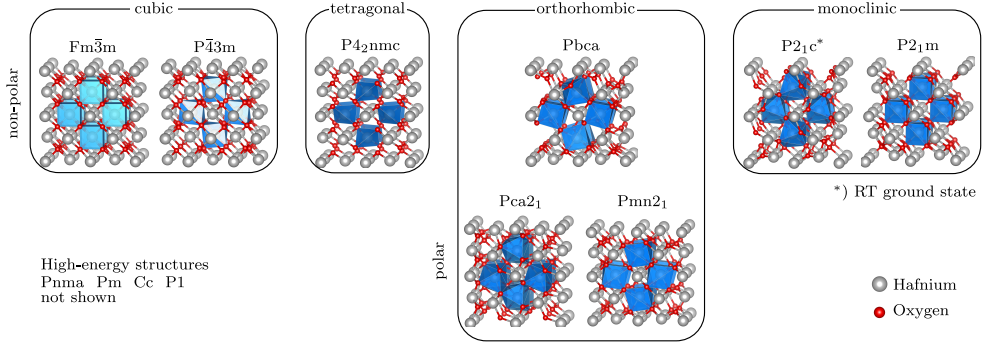

- Gate dielectrics semiconductor devices
- Control rods in nuclear reactors
- Ferroelectricity
- Surprisingly poor understanding of phase diagram

J. Am. Ceram. Soc., **89** [12] 3751–3758 (2006)
DOI: 10.1111/j.1551-2916.2006.01286.x

The Zirconia–Hafnia System: DTA Measurements and Thermodynamic Calculations

Chong Wang, Matvei Zinkevich[†], and Fritz Aldinger[*]

Max-Planck-Institut für Metallforschung and Institut für Nichtmetallische Anorganische Materialien, Universität Stuttgart, Stuttgart, Germany

Table II. Literature Information on the Phase Transition Data of HfO_2 (α, Monoclinic; β, Tetragonal; γ, Cubic; *L*, Liquid)

Transition	Reference	Temperature (K)			Enthalpy of transformation (J/mol)	Entropy of transformation (J·(mol·K)$^{-1}$)	Experimental method
		A_s	M_s	T_0			
α↔β	Curtis *et al.*[26]	1973					HTXRD
	Wolten[6]	1883	2013	1948			HTXRD
	Aldebert *et al.*[24]	1773	1823	1798			HTXRD
	Fujimori *et al.*[18]	2113	2063	2088			Dilatometry
	Boganov *et al.*[27]	2173					HTXRD
	Ruh *et al.*[11]			1893			HTXRD
	Senft and Stubican[22]			2023±20			HTXRD
	Stacy *et al.*[23]			2038			ND
	Stacy and Wilder[25]	2023	2073	2048			HTXRD
	Ruh and Hollenberg[28]	1863					HTXRD
	Stansfield[19]	2073					DTA
	Gulamova and Novoselova[21]		2066±40				HTXRD
	Kasper and Troyanchuk[5]			2023±20			HTXRD
	Shevchenko *et al.*[14]	2103	2083	2093			DTA
	Kuznetsov *et al.*[20]	2073					HTXRD
	Baun[17]	2080 (A_f)	2018				RS
	This work	2066	2038	2052			DTA, extrapolated
	Boganov *et al.*[27]	2973					HTXRD
	Kasper and Troyanchuk[5]	2873					DTA
	Shevthenko and Lopato[29]	2803					DTA

Effective harmonic potentials

$$F_{\text{harm}}[\{\mathbf{a}_i\}, T] = \sum_{n\mathbf{q}} \left(\frac{\hbar\omega_{n\mathbf{q}}}{2} + k_B T \ln\left[1 - e^{-\frac{\hbar\omega_{n\mathbf{q}}}{k_B T}}\right] \right)$$

Determine the best harmonic approximation for the part of the potential energy surface which dominates nuclear motion at given conditions (Hooton, 1955)

Variational formulation

$$F[\hat{U}, \hat{\rho}_0] \leq \mathcal{F}_{\text{EHP}} = \underbrace{F[\hat{\mathcal{U}}, \hat{\rho}]}_{F_{\text{harm}}} + \underbrace{\text{Tr}\left[\hat{\rho}(\hat{U} - \hat{\mathcal{U}})\right]}_{F_{\text{corr}}}$$

$$F_{\text{corr}}[\{\mathbf{a}_i\}, T] = \int \rho\left(E_{pot} - E_{HA}\right) \mathrm{d}\boldsymbol{R}$$

Errea, Calandra, Mauri *Phys. Rev. Lett.* 111 (2013) 177002

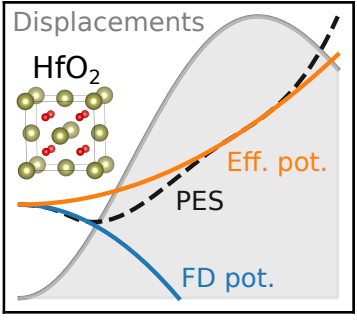

HfO_2: Effective harmonic potential with machine-learned force field

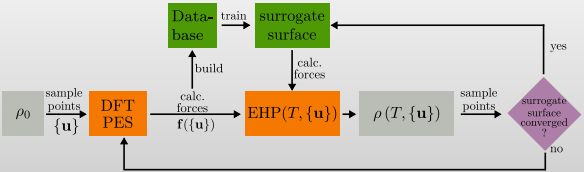

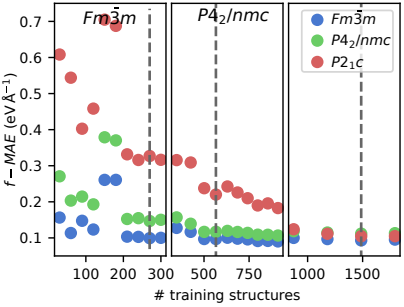

Bichelmaier, Carrete, Madsen *Phys. Rev. B* 107 (2023) p184111

HfO_2 Thermal expansion

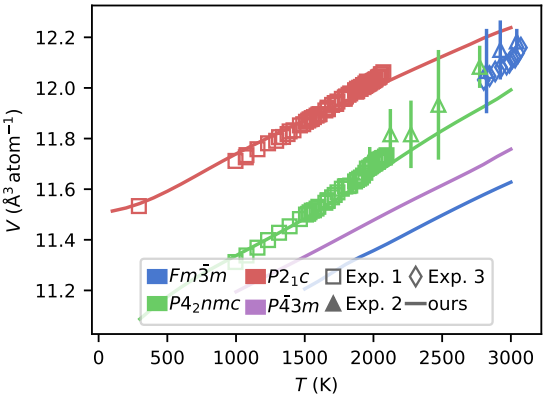

- Approx. $3 \cdot 10^6$ structures evaluated
- Excellent agreement of temperature dependence of lattice constants
- Not for cubic phases

Bichelmaier, Carrete, Madsen *Phys. Rev. B* 107 (2023) p184111

HfO_2 Free energies

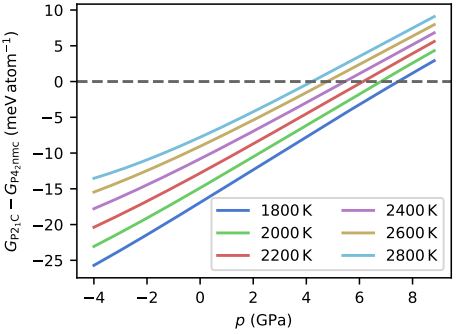

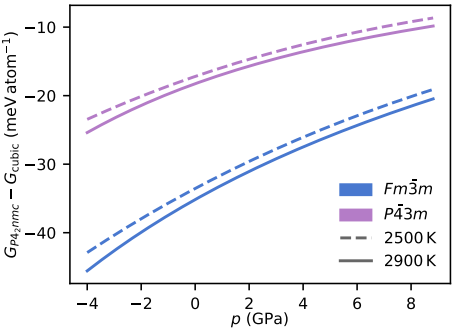

- Phase transition $P2_1c$ – $P4_2nmc$
- Cubic phases not stable
  - Few experiments with internal disagreement
  - Presence of oxygen vacancies ?
  - Multiple results suggest that no stoichiometric cubic phase exits in ZrO_2

Bichelmaier, Carrete, Madsen *Phys. Rev. B* 107 (2023) p184111

Outline

- Neural-network force fields
- Effective harmonic potentials
  - Phase stability in HfO_2
- The $SrTiO_3$ surface phase diagram
- Nested sampling
  - The phase diagram of Si

$SrTiO_3$(110) surface phase diagram

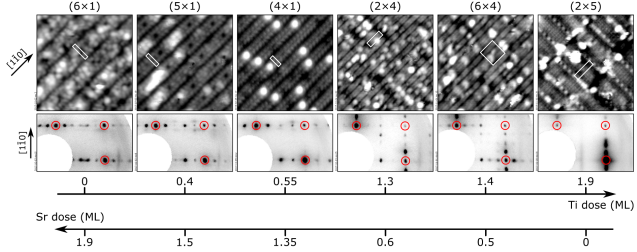

Riva et al., *Phys. Rev. Mater.* 3 (2019) 043802

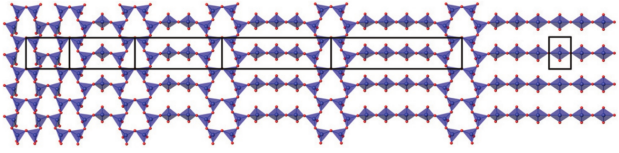

Enterkin et al., *Nat. Mater.* 9 (2010) 245
see also Wang et. al. *Phys. Rev. B* 90 (2014) 035436

The Covariance Matrix Adaptation - Evolution Strategy

- ESs commonly employed for continuous-parameter optimisation
- Employ lower variety of genetic operators than GA
- Endogenous parameters define the genotype distribution and are adapted during evolution

GitHub: Clinamen2

CMA-ES

- Population drawn from multi-dimensional normal distribution

$$\mathbf{x}_k^{(g)} \sim \mathcal{N}\left(\mathbf{m}^{(g)}, (\sigma^{(g)})^2 \mathbf{C}^{(g)}\right)$$

- Transferable hyperparameters
- Problem-dependent parameters: $\sigma^{(0)}$, $\mathbf{m}^{(0)}$

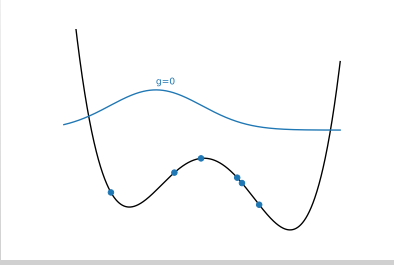

N. Hansen, arXiv:1604.00772
Arrigoni et al. *npj Comput. Mater.* 7 (2021) 71
Wanzenböck et al. *Comput. Phys. Commun.* 297 (2024) 109065

The Covariance Matrix Adaptation - Evolution Strategy

- ESs commonly employed for continuous-parameter optimisation
- Employ lower variety of genetic operators than GA
- Endogenous parameters define the genotype distribution and are adapted during evolution

GitHub: Clinamen2

CMA-ES

- Population drawn from multi-dimensional normal distribution

$$\mathbf{x}_k^{(g)} \sim \mathcal{N}\left(\mathbf{m}^{(g)}, (\sigma^{(g)})^2 \mathbf{C}^{(g)}\right)$$

- Transferable hyperparameters
- Problem-dependent parameters: $\sigma^{(0)}$, $\mathbf{m}^{(0)}$

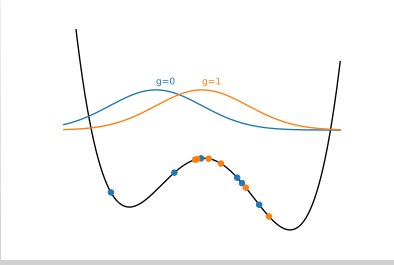

N. Hansen, arXiv:1604.00772
Arrigoni et al. *npj Comput. Mater.* 7 (2021) 71
Wanzenböck et al. *Comput. Phys. Commun.* 297 (2024) 109065

The Covariance Matrix Adaptation - Evolution Strategy

- ESs commonly employed for continuous-parameter optimisation
- Employ lower variety of genetic operators than GA
- Endogenous parameters define the genotype distribution and are adapted during evolution

GitHub: Clinamen2

CMA-ES

- Population drawn from multi-dimensional normal distribution

$$\mathbf{x}_k^{(g)} \sim \mathcal{N}\left(\mathbf{m}^{(g)}, (\sigma^{(g)})^2 \mathbf{C}^{(g)}\right)$$

- Transferable hyperparameters
- Problem-dependent parameters: $\sigma^{(0)}$, $\mathbf{m}^{(0)}$

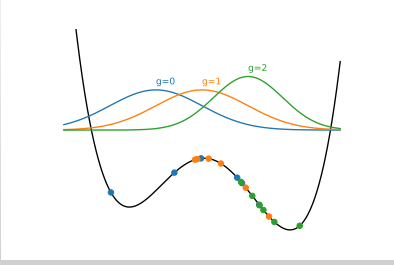

N. Hansen, arXiv:1604.00772
Arrigoni et al. *npj Comput. Mater.* 7 (2021) 71
Wanzenböck et al. *Comput. Phys. Commun.* 297 (2024) 109065

The Covariance Matrix Adaptation - Evolution Strategy

- ESs commonly employed for continuous-parameter optimisation
- Employ lower variety of genetic operators than GA
- Endogenous parameters define the genotype distribution and are adapted during evolution

GitHub: Clinamen2

CMA-ES

- Population drawn from multi-dimensional normal distribution

$$\mathbf{x}_k^{(g)} \sim \mathcal{N}\left(\mathbf{m}^{(g)}, (\sigma^{(g)})^2 \mathbf{C}^{(g)}\right)$$

- Transferable hyperparameters
- Problem-dependent parameters: $\sigma^{(0)}$, $\mathbf{m}^{(0)}$

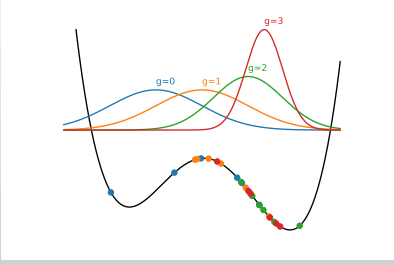

N. Hansen, arXiv:1604.00772
Arrigoni et al. *npj Comput. Mater.* 7 (2021) 71
Wanzenböck et al. *Comput. Phys. Commun.* 297 (2024) 109065

Surface reconstructions with CMA-ES

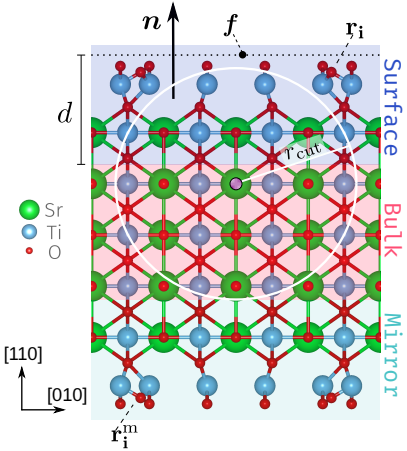

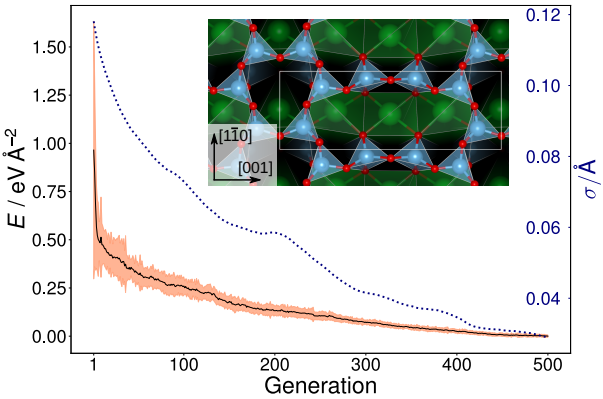

- Adapt CMA-ES to surface reconstructions
- 42 atoms → 126 dof (**4 × 1**)
- DFT backend reproduces 6-10 overlayer from literature

Training NNFF on CMA-ES trajectory

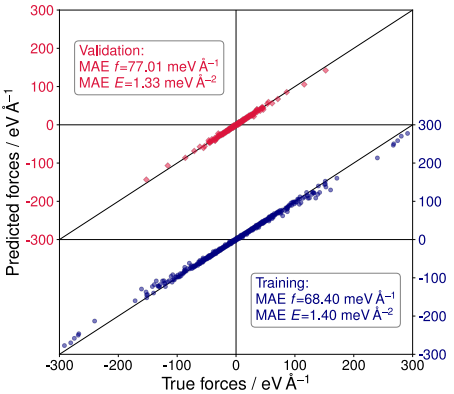

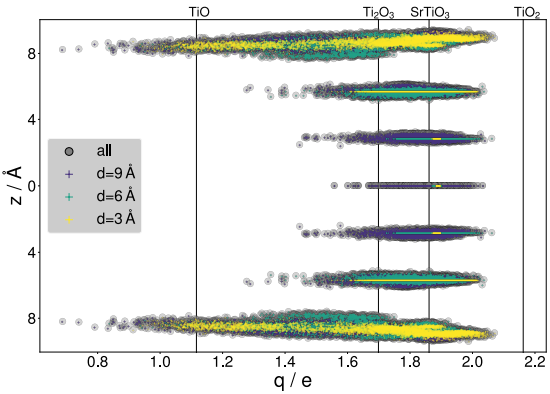

- Good agreement with DFT over large range of energies/forces
- Diverse set of training structures with net atomic charges covering known titanium oxidation states.

Wanzenböck et al. Digital Discovery, 1 (2022) p703

Sets of CMA-ES runs with NNFF backend

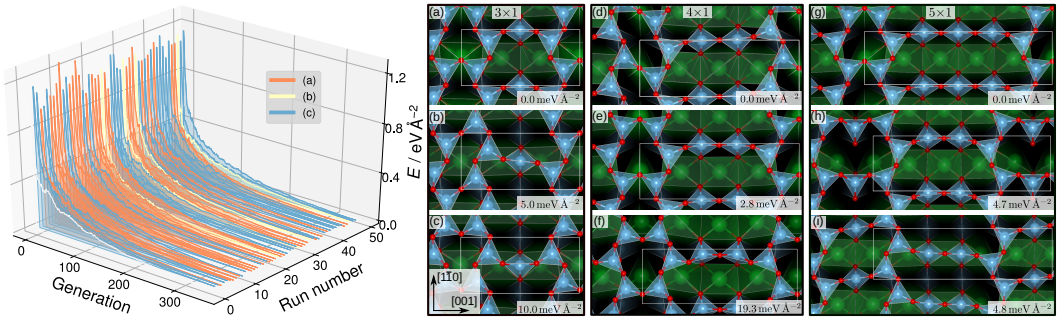

- Set of 50 runs. Same founder; Different random seeds
- 4 × 1: *P*2 structure energetically comparable to *Pm* structure
- 4 × 1 training data.

Wanzenböck et al. Digital Discovery, 1 (2022) p703

STO(110) 4 × 1 - STM

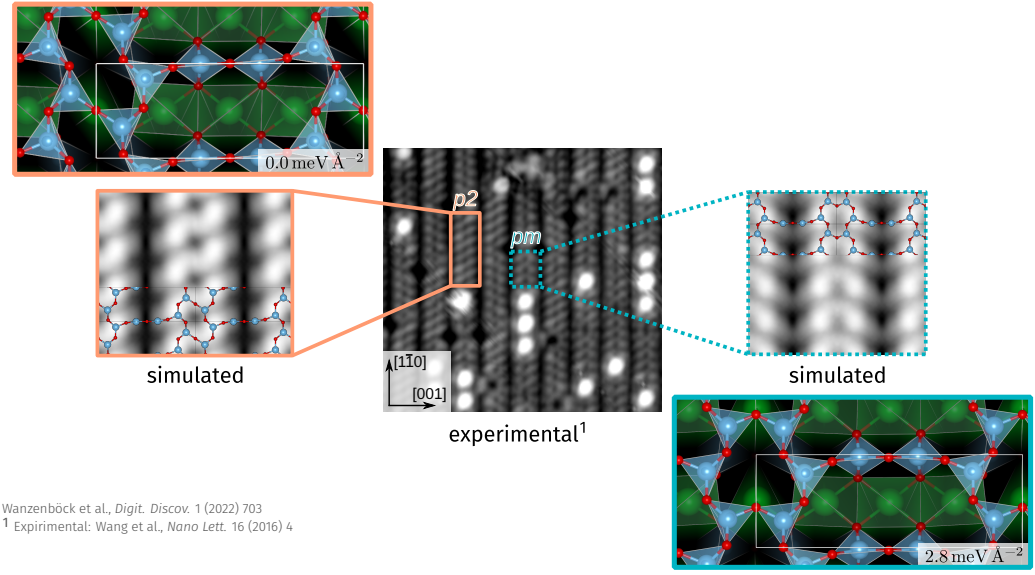

Wanzenböck et al., *Digit. Discov.* 1 (2022) 703

[1] Expirimental: Wang et al., *Nano Lett.* 16 (2016) 4

Learning in High Dimension Always Amounts to Extrapolation

Randall Balestriero[1], Jérôme Pesenti[1], and Yann LeCun[1,2]

[1]Facebook AI Research, [2]NYU

The notion of interpolation and extrapolation is fundamental in various fields from deep learning to function approximation. Interpolation occurs for a sample $\boldsymbol{x}$ whenever this sample falls inside or on the boundary of the given dataset's convex hull. Extrapolation occurs when $\boldsymbol{x}$ falls outside of that convex hull. One fundamental (mis)conception is that state-of-the-art algorithms work so well because of their ability to correctly interpolate training data. A second (mis)conception is that interpolation happens throughout tasks and datasets, in fact, many intuitions and theories rely on that assumption. We empirically and theoretically argue against those two points and demonstrate that on any high-dimensional (>100) dataset, interpolation almost surely never happens. Those results challenge the validity of our current interpolation/extrapolation definition as an indicator of generalization performances.

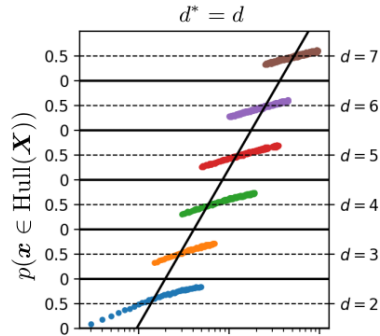

$$\boldsymbol{x}_i \sim \mathcal{N}(0, I_d)$$

PCA fingerprints.

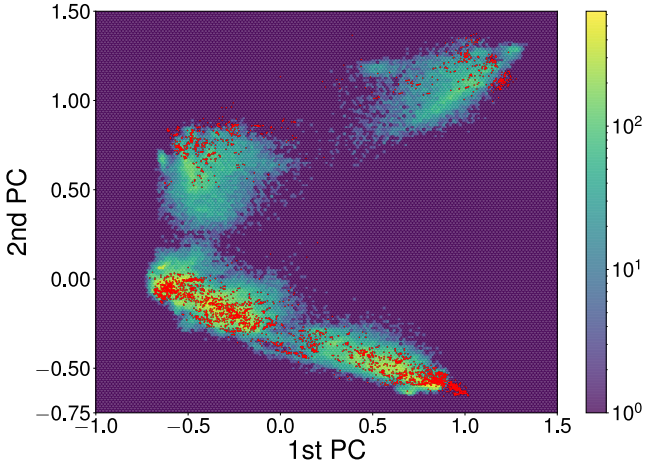

Similarity: The projection of the local atomic environments of the low energy **5 × 1** structures fall within the area covered by the projection of the **4 × 1** training data.

Wanzenböck et al. Digital Discovery, 1 (2022) p703

STO(110) 2 × *m*

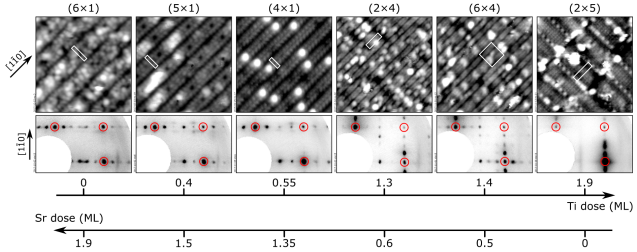

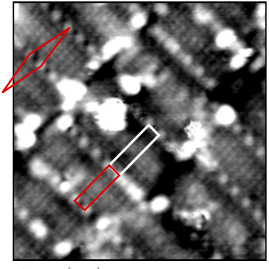

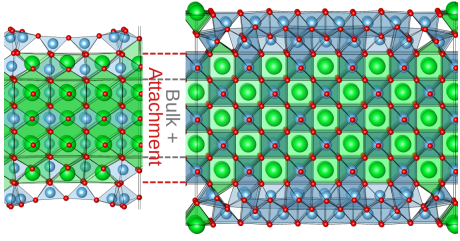

Wang et al. *Nano Lett.* 16 (2016) 4
Riva et al., *Phys. Rev. Mater.* 3 (2019) 043802

Active learning with neuralIL

Uncertainty estimation

- Deep ensembles
- Committees

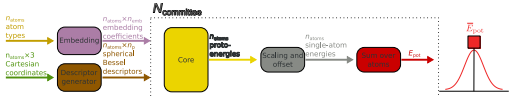

Versatile Learned Optimization

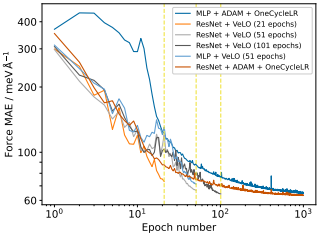

Optimize adversarial loss (Koda-Bombarelli)

$$\mathcal{L} = \sigma_f^2 \exp\left(-\frac{E_{\text{pot}}}{k_B T}\right)$$

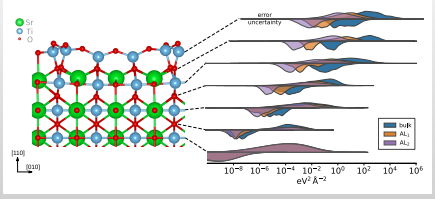

Carrete et al. *J. Chem. Phys.* 158, 204801 (2023)

STO(110) 2 × *m*: MLFF driven EA

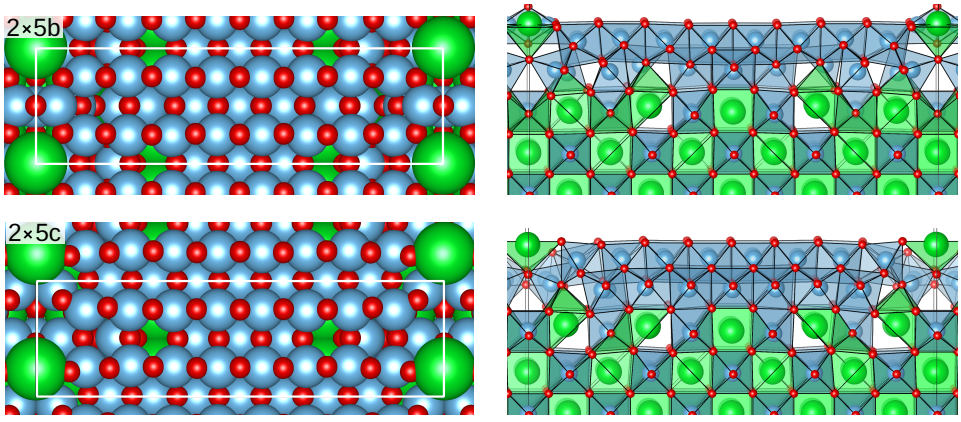

- 158 atoms: 474 DOF
- Identify several local minima
- New structure in agreement with published STM

Outline

- Neural-network force fields
- Effective harmonic potentials
  - Phase stability in HfO_2
- The $SrTiO_3$ surface phase diagram
- Nested sampling
  - The phase diagram of Si

Skilling's nested sampling

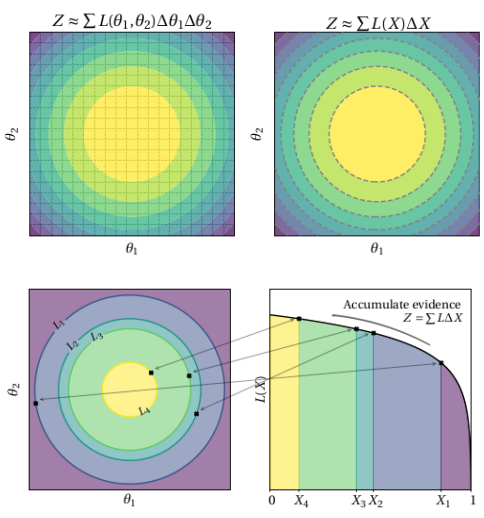

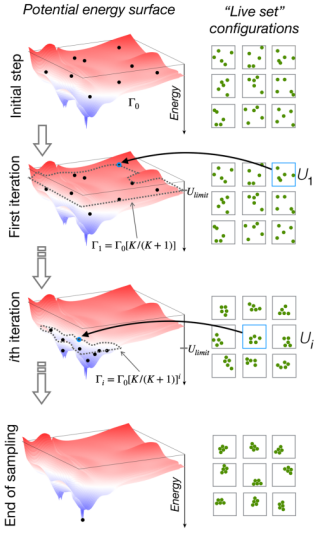

Ashton et al *Nature Rev. Methods Primers* 2 (2022) 39

Pártay et al *Eur. Phys. J. B* 94 (2021) 159

Silicon. The NNFF

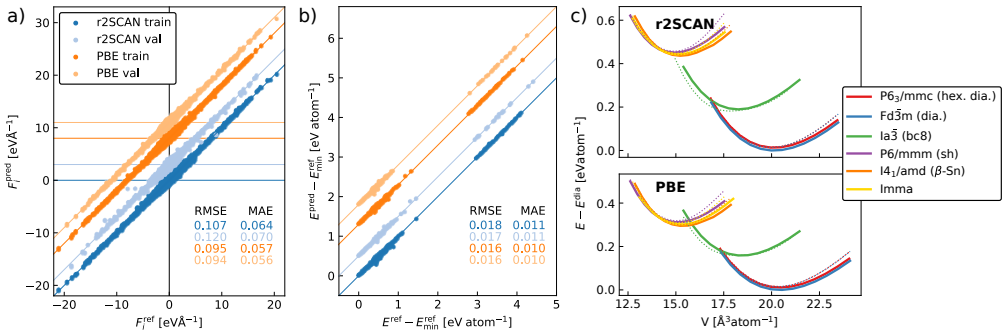

- Structures taken from database of Bartók-Csányi and recalculated with PBE and r2SCAN
- r2SCAN results in increase in energy differences

Unglert, Carrete, Pártay, Madsen. *Phys. Rev. Mater.* 7, (2023) 123804

Silicon. The phase diagram

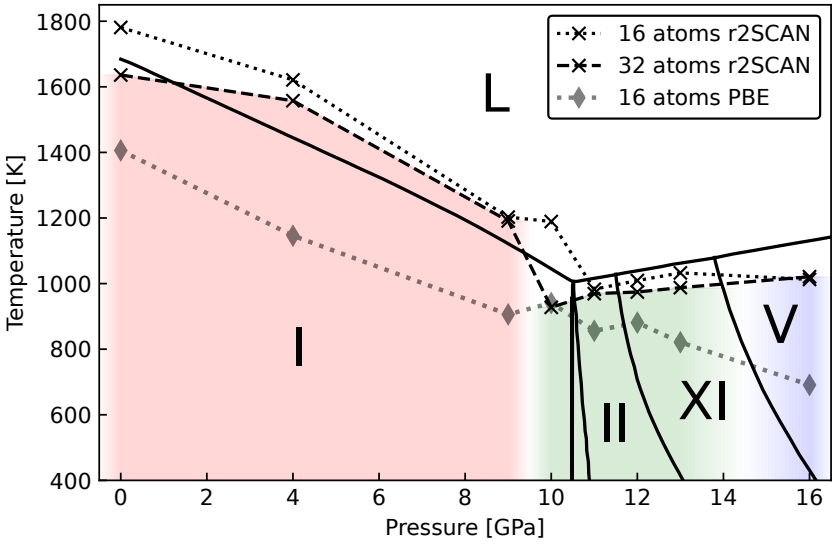

Unglert, Carrete, Pártay, Madsen. *Phys. Rev. Mater.* 7, (2023) 123804

Silicon. The nested sampling walkers

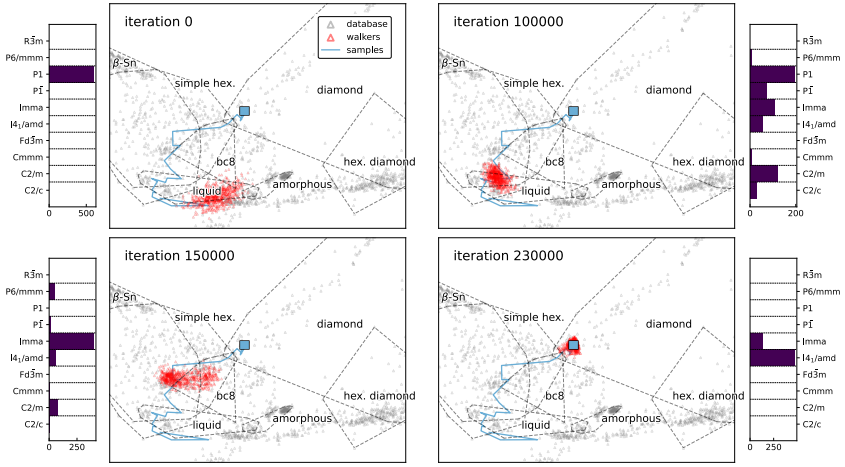

- Highly diverse training set is essential

Unglert, Carrete, Pártay, Madsen. *Phys. Rev. Mater.* 7, (2023) 123804

Silicon. The basins

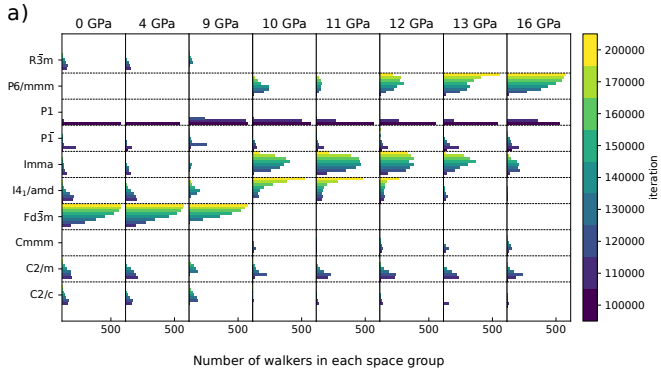

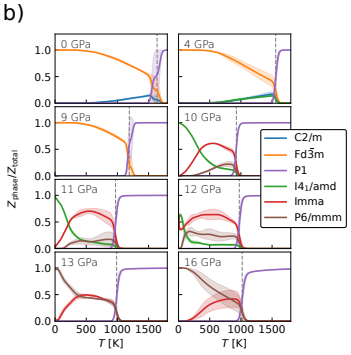

Unglert, Carrete, Pártay, Madsen. *Phys. Rev. Mater.* 7, (2023) 123804